PCT

WORLD INTELLECTUAL PROPERTY ORGANIZATION
International Bureau

INTERNATIONAL APPLICATION PUBLISHED UNDER THE PATENT COOPERATION TREATY (PCT)

(51) International Patent Classification 6 :
H04L 25/03, 25/497

A1

(11) International Publication Number: WO 98/52330

(43) International Publication Date: 19 November 1998 (19.11.98)

(21) International Application Number: PCT/IB97/00554

(22) International Filing Date: 15 May 1997 (15.05.97)

(71) Applicant (*for all designated States except US*): INTERNATIONAL BUSINESS MACHINES CORPORATION [US/US]; Old Orchard Road, Armonk, NY 10504 (US).

(72) Inventors; and
(75) Inventors/Applicants (*for US only*): COKER, Jonathan, Darrel [US/US]; 1605 5th Street Northeast, Rochester, MN 55901 (US). ELEFTHERIOU, Evangelos, Stavros [GR/CH]; Bellariastrasse 53, CH-8038 Zurich (CH). GALBRAITH, Richard, Leo [US/US]; 2232 N.W. 52 Street, Rochester, MN 55901 (US). HIRT, Walter [CH/CH]; Hinderweidstrasse 29, CH-8907 Wettswil (CH).

(74) Agent: HEUSCH, Christian; International Business Machines Corporation, Saeumerstrasse 4, CH-8803 Rueschlikon (CH).

(81) Designated States: JP, US, European patent (AT, BE, CH, DE, DK, ES, FI, FR, GB, GR, IE, IT, LU, MC, NL, PT, SE).

Published
With international search report.

(54) Title: APPARATUS AND METHOD FOR NOISE-PREDICTIVE MAXIMUM LIKELIHOOD DETECTION

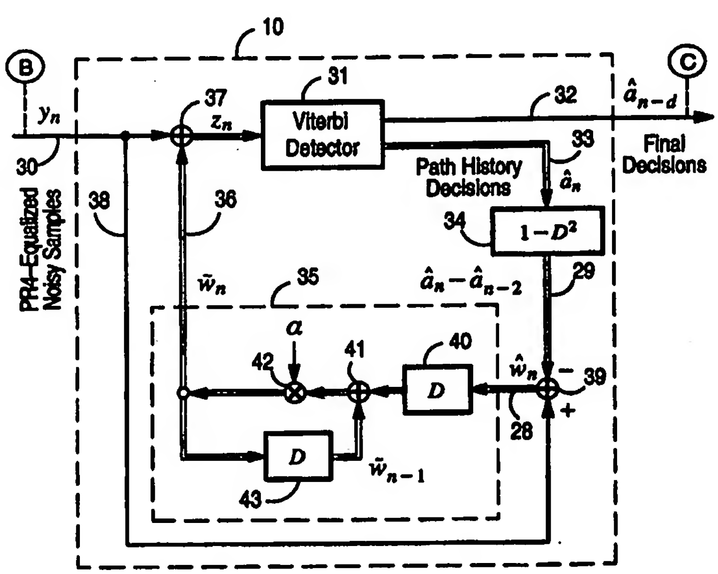

(57) Abstract

In a maximum likelihood sequence detector for symbol sequences which were equalized in a PR4 equalizer, noise prediction means (35) are provided including infinite impulse response (IIR) filtering, which have noise-whitening capabilities and are imbedded into the maximum likelihood detection process. The resulting INPML detector (10) can be implemented in digital or analog circuit technoology. In addition, a DC-notch filter (44a) and a stochastic gradient procedure can be provided for DC offset compensation and for MR head or signal asymmetry compensation.

DESCRIPTION

APPARATUS AND METHOD FOR NOISE–PREDICTIVE MAXIMUM LIKELIHOOD DETECTION

TECHNICAL FIELD

Present invention relates to data detection apparatus and methods. It is in particular applicable to direct access storage (DASD) devices using partial–response (PR) signaling and maximum likelihood sequence detection (MLSD).

BACKGROUND OF THE INVENTION

In DASD systems as well as in data transmission systems, the signal read from the storage device or received at the output of a transmission channel has to be converted in the receiver into a sequence of symbols which most likely represents the data (symbol) sequence initially stored or transmitted by the sender, despite interference between adjacent symbols, and despite added noise.

The optimum receiver for detecting an uncoded data sequence in the presence of intersymbol interference (ISI) and noise consists of a whitened–matched filter followed by a Viterbi detector which performs maximum likelihood sequence detection on the ISI trellis. In PRML (Partial–Response Maximum Likelihood) systems the composite noise at the input of the detector is not white, resulting in sub–optimal performance. This sub–optimality is more pronounced at high recording densities since the linear PR4 (PR class 4) equalizer tends to enhance the electronic noise component of the composite noise at the input of the PRML detector. In addition to colored noise, nonlinear distortion due to nonlinear bit–shift and head asymmetry could further degrade performance of PRML systems.

International Patent Application PCT/WO97/11544 (IBM) discloses a scheme for data detection in a direct access storage device, called NPML (Noise–Predictive Maximum Li-

kelihood detection), that arises by imbedding a noise prediction/whitening filter into the branch metric computation of the Viterbi detector. It has been shown via simulations that the NPML detectors offer substantial performance gains over the PRML detectors.

However, implementation of the imbedded predictor/whitener as a bank of finite–impulse–response (FIR) filters or equivalent table look–up operations, e.g. by means of random access memory (RAM), demands a certain level of complexity of the NPML hardware realization. A further difficulty with presently available implementation technologies is the time constraint imposed by high speed clock requirements.

Application of the Viterbi algorithm to channels represented by an IIR (Infinite Impulse Response) discrete–time equivalent model has been studied in a publication by A. Duel–Hallen et al. "Delayed decision–feedback sequence estimation," *IEEE Trans. Commun.*, COM–37, pp.428–436, May 1989. The approach in that reference assumes a decision feedback equalization prefilter whose feedback filter is an IIR filter combined with Viterbi detection. In contrast, the present invention considers a forward partial–response or generalized partial–response linear equalizer and a noise whitening IIR predictor imbedded into the Viterbi detector.

OBJECTS OF THE INVENTION

It is a main object of present invention to provide a more efficient and simpler realization of the noise prediction/whitening mechanism for a NPML detector.

It is a further object of the invention to devise a partial–response maximum likelihood detection scheme that utilizes past decisions from the path memory of the Viterbi detector for the noise prediction process.

Another object of the invention is to enable additional mechanisms for a maximum likelihood detector which allow compensation of reading head asymmetries and of DC offset in the receiver.

SUMMARY OF THE INVENTION

The invention provides a partial–response signaling, maximum likelihood detector with an infinite impulse response (IIR) noise predictor and whitening filter imbedded in the Viterbi detector (INPML). As an additional feature, a DC (zero frequency) notch filter may be provided for DC offset compensation. Furthermore, an additional compensation method can be provided that is imbedded in the branch metric computation of the INPML detector for dynamic signal–asymmetry and DC offset compensation.

Advantages of the invention are that, besides its simplicity in implementation, it does not compromise performance of the detector. It has the further important advantage that it can be "piggy–backed" on existing PRML systems so that there is no need for development and implementation of an entirely new channel architecture which would be a complex and costly task. The addition of a DC–notch filter or DC compensation method renders the INPML detector completely immune to DC offset, tolerant and robust against various types of non–linearity and in particular head asymmetry, and tolerant to thermal asperities, which is a further impairment in digital magnetic recording systems.

In the following, embodiments of the invention are described with reference to the drawings .

LIST OF DRAWINGS

Fig. 1 is a block diagram of a PRML detector in which present invention can be implemented.

Fig. 2A is a block diagram of the maximum likelihood detector according to the invention with a single–pole imbedded IIR noise predictor .

Fig. 2B shows an alternative, equivalent implementation of the IIR noise predictor for the inventive maximum likelihood detector of Fig. 2A.

Fig. 3 shows the 4–state trellis for the INPML detector of Fig. 2A.

Fig. 4 is a block diagram of an alternative maximum likelihood detector in accordance with the invention in which an imbedded IIR noise predictor with 2 poles and 2 zeros is provided.

Fig. 5 shows the bit error probability for various ML detectors including the INPML detector of the invention for a channel with the normalized linear recording density $PW50/T \approx 2.86$.

Fig. 6 shows the relative SNR for a given bit error probability, also for various ML detectors including INPML (4 states), as a function of $PW50/T$.

Fig. 7A is a block diagram of an inventive INPML detector with an additional, imbedded DC–notch filter.

Fig. 7B schematically shows a first arrangement of an INPML detector with a cascaded DC–notch filter (between equalizer and detector).

Fig. 7C schematically shows a second arrangement of an INPML detector with a cascaded DC–notch filter (preceding the equalizer).

Fig. 8 illustrates a RAM based dynamic non–linearity estimation to be used for DC offset and head asymmetry compensation.

Fig. 9 shows the bit error probability for the INPML detector with and without asymmetry estimation (channel $PW50/T \approx 2.86$).

DETAILED DESCRIPTION

Fig. 1 is the block diagram of a known PRML channel architecture for a data recording system. Such a system was also described in the above mentioned International Patent Application PCT/WO97/11544.

Customer data I_n are written in the form of binary digits $a_n \in \{-1, +1\}$ by write head 15 on the disk 11 after being encoded in an encoder 12 by a rate–8/9 RLL (Run Length Limited) code and serialized in a serializer 13 and precoded in a precoder 14 by a $\frac{1}{1 \oplus D^2}$ operation where D is the unit delay operator and $\oplus$ means addition modulo 2. When receiving

the customer data from said disk 11, an analog signal r(t) is generated by the read head 15 and provided at the read head's output. The signal r(t) is then applied via arm electronic circuitry 16 to a variable gain amplifier (VGA) circuit 17. The output signal of the the VGA circuit 17 is first low–pass filtered using an analog low–pass filter 18 (LPF) and then converted to a digital form x_n by an analog–to–digital (A/D) converter 19. The functions of the A/D converter 19 and VGA amplifier 17 are controlled by the timing recovery and gain control loops 20/26 and 21/26, respectively. The analog low–pass filter 18 is preferably a filter which boosts the higher frequencies to avoid saturation of the A/D converter 19 and to support the digital equalizer 22. The digital samples x_n at the output of the A/D converter 19 (line labeled A in Fig. 1) are first shaped to PR4 signal samples by the digital equalizer 22 (line labeled B in Fig. 1) and are then passed on to a maximum likelihood detector circuitry 10 (ML detector) in the form of digital noisy samples y_n. The output data of the ML detector 10 (i.e. the final decisions on the line labeled C in Fig. 1), after inverse precoding by means of an inverse precoder 23 performing a $1 \oplus D^2$ operation, are fed via a deserializer 24 to a rate 9/8 decoder 25 for the rate–8/9 RLL code which delivers the retrieved customer data $\hat{I}_{n-d}$. The inverse precoder function 23 following the ML detector in Fig. 1 can be a separate functional block (as shown) or it can be imbedded in the trellis (survivor path memory) of the ML detector.

In the above mentioned International Patent Application PCT/WO97/11544, the maximum likelihood detector 10 was a noise–predictive maximum likelihood detector (NPML detector) which uses a finite impulse response (FIR) filter/predictor to estimate the noise contents of the input signals.

First Embodiment of Invention:

Present invention provides an improvement for the maximum likelihood detector portion of a PRML data recording channel. Its principles are shown in the block diagram of Fig. 2A which represents the ML detector portion 10 of Fig. 1. The PR4–equalized samples y_n appearing on line 30 (marked B) are modified by the noise prediction process according to the invention, fed as samples z_n to the Viterbi detector 31 which on its output 32 delivers the recovered data symbols $\hat{a}_{n-d}$, which are the delayed final decisions (marked C) of the

Viterbi detector. Preliminary symbols (path history decisions) $\hat{a}_n$ are delivered on an output 33 of the Viterbi detector. These preliminary symbols are fed to a reconstruction means 34 having transfer function $1 - D^2$, to obtain on line 29 a reconstructed sample sequence $(\hat{a}_n - \hat{a}_{n-2})$. This reconstructed sample sequence is subracted in subtracting means 39 from the noisy equalized samples y_n appearing on branch line 38, to obtain noise samples $\hat{w}_n$ on line 28. These noise samples $\hat{w}_n$ are fed to noise predictor circuit 35 which is an infinite impulse response (IIR) filter. The predicted noise samples $\tilde{w}_n$ appearing on output line 36 are combined in circuit 37 with the noisy samples y_n to provide samples z_n for input to the Viterbi detector 31. Note that the noise prediction and metric update operations are performed separately for each state using decisions from the corresponding path memory. These per state operations in the resulting INPML detector are symbolized in Fig. 2 by double signal flow lines.

The IIR predictor 35 of present preferred embodiment is a single–pole device. It receives the noise samples $\hat{w}_n$ on line 28, which then are delayed in unit delay means 40. Its output, after combination with a delayed noise signal (output of unit delay means 43) in adder 41 and multiplication by a coefficient α in multiplication means 42, provides the desired noise signal $\tilde{w}_n$ on line 36. The IIR noise predictor 35 executes the transfer function $\alpha D/(1 - \alpha D)$.

Thus, the noise predictor is an infinite impulse response device which is imbedded (for each state) into the maximum likelihood detection arrangement, as shown in Fig. 2A. This arrangement will be termed INPML detector in the following (for "Infinite Impulse response Noise Predictive Maximum Likelihood" detector). Its operation is described in the sequel.

Let y_n be the output of the PR4 digital equalizer, line labeled B in Fig. 1 and Fig. 2A. This output then consists of a PR4 data signal, with noiseless nominal values of $-2,\ 0,\ +2$, and colored noise, i.e.,

$$y_n = a_n - a_{n-2} + w_n \tag{1}$$

where $a_n \in \{-1, +1\}$ denotes the encoded/precoded data sequence written on the magnetic medium with a rate $1/T$ and w_n represents the colored noise sequence at the

output of the digital partial–response equalizer (T is the channel encoded bit time interval and subscript n indicates time instant nT). The power of the colored noise component w_n in (1) can be reduced by noise prediction.

Figure 2A shows the basic concept of a single coefficient IIR predictor imbedded into the Viterbi detector. The basic principle can be explained as follows. Let

$$E(D) = \frac{1}{1 - aD} \quad , \qquad a < 1 \tag{2}$$

denote the D–transform of the single–pole IIR prediction error (whitening) filter. Then, assuming ideal path history decisions $\hat{a}_n$, i.e., $\hat{w}_n = w_n$ on line 28, the D–transform of the whitened noise sequence at the output of $E(D)$ is given by

$$e(D) = \frac{1}{1 - aD} w(D) = [1 + P(D)]\, w(D) = w(D) + \tilde{w}(D) \quad , \tag{3}$$

with

$$P(D) = \frac{aD}{1 - aD} \; . \tag{4}$$

$w(D)$ in (3) represents the D–transform of the colored noise sequence in (1) and $\tilde{w}(D)$ denotes its predicted value through the single–pole prediction filter. In the time domain $\tilde{w}(D)$ satisfies the following recursive equation

$$\tilde{w}_n = a(\tilde{w}_{n-1} + w_{n-1}) = a\, \tilde{w}_{n-1} + a\, (y_{n-1} - a_{n-1} + a_{n-3}) = a\, e_{n-1} \quad . \tag{5}$$

The single–pole IIR predictor filter 35 described by (4) and (5) and shown in Fig. 2A can also be implemented as shown in Fig. 2B. This IIR predictor 35b also receives noise samples $\hat{w}_n$ on line 28. They are combined in adder 41 with predicted noise samples $\tilde{w}_n$, then delayed by unit delay element (D) 40b and then multiplied in multiplication means 42 by a coefficient a, to provide predicted noise samples $\tilde{w}_n$ on output line 36.

Equation (5) and PR4 signalling define a 4–state ML detector which encompasses a single–pole IIR predictor. If s_j, $j = 0, 1, 2, 3$, denotes the j–th state (a_{n-1}, a_{n-2}) of the

4–state PR4 trellis then, in view of (1) and (3), the branch metric at time nT of the Viterbi detector corresponding to the state transition $s_j \rightarrow s_k$ takes the form

$$\lambda_n(s_j, s_k) = \left[y_n - a_n + a_{n-2}(s_j) + \tilde{w}_n(s_j)\right]^2 = \left[e_n(s_j, s_k)\right]^2 \quad , \qquad (6)$$

where a_n and $a_{n-2}(s_j)$ are determined by the hypothesized state transition $s_j \rightarrow s_k$ and $\tilde{w}_n(s_j)$ is the predicted noise sample associated with state s_j. In particular, the reconstructed PR4 samples $(a_{n-1} - a_{n-3})$ in (5) are replaced in practice by $(\hat{a}_{n-1} - \hat{a}_{n-3})$ which are obtained from the path memory of the Viterbi detector associated with state s_j.

The 4–state INPML detector with a single–pole IIR predictor/whitening filter operates on the trellis shown in Figure 3. Every state at time instant nT is associated with :

– State Metrics: $J_n(0)$, $J_n(1)$, $J_n(2)$, $J_n(3)$,

– Noise Estimates: $\tilde{w}_n(0)$, $\tilde{w}_n(1)$, $\tilde{w}_n(2)$, $\tilde{w}_n(3)$.

The branch metrics shown on the trellis branches of Figure 5 are computed as follows:

$$\begin{aligned}
\lambda_n(0,0) &= |\, e_n(0,0) \,|^2 &&\text{, where} & e_n(0,0) &= y_n + \tilde{w}_n(0) \\
\lambda_n(1,0) &= |\, e_n(1,0) \,|^2 &&\text{, where} & e_n(1,0) &= y_n + 2 + \tilde{w}_n(1) \\
\lambda_n(2,1) &= |\, e_n(2,1) \,|^2 &&\text{, where} & e_n(2,1) &= y_n + \tilde{w}_n(2) \\
\lambda_n(3,1) &= |\, e_n(3,1) \,|^2 &&\text{, where} & e_n(3,1) &= y_n + 2 + \tilde{w}_n(3) \\
\lambda_n(0,2) &= |\, e_n(0,2) \,|^2 &&\text{, where} & e_n(0,2) &= y_n - 2 + \tilde{w}_n(0) \\
\lambda_n(1,2) &= |\, e_n(1,2) \,|^2 &&\text{, where} & e_n(1,2) &= y_n + \tilde{w}_n(1) \\
\lambda_n(2,3) &= |\, e_n(2,3) \,|^2 &&\text{, where} & e_n(2,3) &= y_n - 2 + \tilde{w}_n(2) \\
\lambda_n(3,3) &= |\, e_n(3,3) \,|^2 &&\text{, where} & e_n(3,3) &= y_n + \tilde{w}_n(3)
\end{aligned} \qquad (7)$$

The state metrics and noise estimates at the next time instant $(n + 1)T$ are computed as follows:

$$J_{n+1}(0) = min\ \{\ J_n(0) + \lambda_n(0,0)\ ,\ J_n(1) + \lambda_n(1,0)\ \}$$

$$\tilde{w}_{n+1}(0) = \begin{cases} a\ e_n(0,0) \\ or \\ a\ e_n(1,0) \end{cases}$$ Depending on whether state 0 or state 1 was the previous "winning" state

$$J_{n+1}(1) = min\ \{\ J_n(2) + \lambda_n(2,1)\ ,\ J_n(3) + \lambda_n(3,1)\ \}$$

$$\tilde{w}_{n+1}(1) = \begin{cases} a\ e_n(2,1) \\ or \\ a\ e_n(3,1) \end{cases}$$ Depending on whether state 2 or state 3 was the previous "winning" state

$$J_{n+1}(2) = min\ \{\ J_n(0) + \lambda_n(0,2)\ ,\ J_n(1) + \lambda_n(1,2)\ \}$$

$$\tilde{w}_{n+1}(2) = \begin{cases} a\ e_n(0,2) \\ or \\ a\ e_n(1,2) \end{cases}$$ Depending on whether state 0 or state 1 was the previous "winning" state

$$J_{n+1}(3) = min\ \{\ J_n(2) + \lambda_n(2,3)\ ,\ J_n(3) + \lambda_n(3,3)\ \}$$

$$\tilde{w}_{n+1}(3) = \begin{cases} a\ e_n(2,3) \\ or \\ a\ e_n(3,3) \end{cases}$$ Depending on whether state 2 or state 3 was the previous "winning" state

By setting $a = 0$ the INPML detector becomes a conventional 4–state PRML detector.

Second Embodiment of Invention:

An alternative embodiment of the noise predictor in the inventive INPML detector is now described with reference to the block diagram of Fig. 4. In this case the prediction error (whitening) filter includes two poles and two zeros.

The predictor 45 shown in Fig. 4 has the same connections to the other portions of the Viterbi detector as predictor 35 in Fig. 2A: A line 28a (28) transferring noise samples $\hat{w}_n$, and a line 36a (36) for the predicted noise samples $\tilde{w}_n$.

The noise samples $\hat{w}_n$ appearing on input 28a are twice delayed in unit delay elements 47 and 48, then multiplied in multiplier 49 by factor $[-(a_2 + \beta_2)]$, and then combined in

adder unit 50 with "auxiliary" signals on lines 51, 52, and 53 to provide predicted noise samples $\tilde{w}_n$ on line 36a.

The "auxiliary" signals are derived as follows: Signal on line 51 results from multiplying the output of delay unit 47 in multiplier 54 by a factor $[-(\alpha_1+\beta_1)]$. Signal on line 52 results from multiplying predicted noise samples $\tilde{w}_n$, delayed in unit delay means 55, by a factor $[-\alpha_1]$ in a multiplier 56. Signal on line 53 results from multiplying predicted noise sample $\tilde{w}_n$, twice delayed in unit delay means 55 and 57, by a factor $[-\alpha_2]$ in multiplier 58. IIR noise predictor 45 executes the transfer function

$$[-(\alpha_1+\beta_1)D-(\alpha_2+\beta_2)D^2]/[1+\alpha_1 D+\alpha_2 D^2].$$

Let

$$E(D)=\frac{1-\beta_1 D-\beta_2 D^2}{1+\alpha_1 D+\alpha_2 D^2}\quad, \tag{8}$$

denote the D–transform of the two–poles, two–zeros IIR prediction error (whitening) filter. Then, the D–transform of the whitened noise sequence at the output of $E(D)$ is given by

$$e(D)=\frac{1-\beta_1 D-\beta_2 D^2}{1+\alpha_1 D+\alpha_2 D^2}w(D)=[1+P(D)]\,w(D)=w(D)+\tilde{w}(D)\quad, \tag{9}$$

with

$$P(D)=\frac{-(\alpha_1+\beta_1)D-(\alpha_2+\beta_2)D^2}{1+\alpha_1 D+\alpha_2 D^2}\quad. \tag{10}$$

$w(D)$ in (9) represents the D–transform of the colored noise sequence in (1) and $\tilde{w}(D)$ denotes its predicted value through the 2–poles/2–zeros prediction filter. In the time domain $\tilde{w}(D)$ satisfies the following recursive equation

$$\begin{aligned}\tilde{w}_n = & -\alpha_1\tilde{w}_{n-1}-\alpha_2\tilde{w}_{n-2}-(\alpha_1+\beta_1)(y_{n-1}-a_{n-1}+a_{n-3})\\ & -(\alpha_2+\beta_2)(y_{n-2}-a_{n-2}+a_{n-4})\quad.\end{aligned} \tag{11}$$

Equation (11) and PR4 signalling can define a 4-state Viterbi detector which encompasses a 2-zeros/2-poles IIR predictor. If s_j, $j = 0, 1, 2, 3$, denotes the j-th state of the 4-state PR4 trellis then, in view of (1) and (9), the branch metric at time nT of the Viterbi detector corresponding to the state transition $s_j \rightarrow s_k$ takes the form

$$\lambda_n(s_j, s_k) = \left[y_n - a_n + a_{n-2}(s_j) + \tilde{w}_n(s_j)\right]^2 = \left[e_n(s_j, s_k)\right]^2 \quad , \qquad (12)$$

where a_n and $a_{n-2}(s_j)$ are determined by the hypothesized state transition $s_j \rightarrow s_k$ and $\tilde{w}_n(s_j)$ is a noise estimate associated with state s_j. As in the previous embodiment the branch metrics (12) for each state transition can now be computed explicitly from expressions (7) with $\tilde{w}_n(s_j)$ according to (11).

Following the same approach, the recursive equation of a 1-zero/2-poles IIR predictor filter with the corresponding branch metric equation can be readily derived ($\beta_2 = 0$ in (8)). Similarly, the recursive equation of a 2-poles IIR predictor filter with the corresponding branch metric equation can also be obtained ($\beta_1 = 0$ and $\beta_2 = 0$ in (8)).

Performance (Improvement gained by the invention):

For the magnetic recording channel it has been found that in the entire range of $0.5 \leq PW50/T \leq 3.5$ where $PW50$ is the pulse width at the 50% amplitude point of the channel's step response and T is the duration of the channel encoded bit, IIR predictors with at most 2 poles and 2 zeros offer the best possible performance irrespective of the noise source, i.e., electronic noise or disk noise, or a combination thereof. In particular, for $0.5 \leq PW50/T \leq 2.7$ the best possible performance is achieved with an IIR predictor consisting of 2 poles and 1 zero, whereas for $2.7 < PW50/T \leq 3.5$ best possible performance is achieved with an IIR predictor consisting of 2 poles and 2 zeros. If the dominant noise source is electronic noise then an INPML detector with a single-pole IIR predictor offers already substantial performance gains over PRML detectors in a wide range of linear recording densities.

The error performance of a magnetic recording system employing INPML detection has been studied by computer simulation. Figure 5 shows bit error probabilities of simulated 4–state INPML and NPML detectors for the channel model with $PW50/T \approx 2.86$. Curve 2 shows the performance of INPML4 (4–state INPML) with a single–pole predictor; compared to curves 1 (PRML) and 3 (EPRML), a gain in noise margin of 2 dB and 0.5 dB is obtained, respectively. Curve 4 corresponds to 4–state NPML with $N = 4$ predictor coefficients. Compared to curve 3 an additional gain of 0.4 dB is obtained. Finally, curve 5 corresponds to a 4–state INPML detector with a 2–zeros and 2–poles IIR predictor. Compared to curve 4 an additional 0.2 dB is obtained, and compared to PRML 2.7 dB gain is obtained.

Figure 6 shows the relative SNR (Signal–to–Noise Ratio) required to achieve a bit error probability of $P_b = 10^{-5}$ for the 4–state NPML with $N = 4$ predictor coefficients, 4–state INPML with a single–pole IIR predictor, and EPRML, all with respect to a PRML system, as a function of the normalized linear density $PW50/T$ for the Lorentzian channel model. Curve 1 corresponds to our reference PRML system. Curve 2 corresponds to the 8–state EPRML system and curves 3 and 4 correspond to 4–state INPML with a single–pole IIR predictor filter and 4–state NPML/N=4, respectively. We observe that the single–pole INPML system is very close in performance to the NPML system and that both provide superior performance compared to all the other systems at any linear recording density.

Further Improvements (Additional Features):

(a) Including a Notch Filter :

Further improvement of the invented INPML detector described so far can be achieved by incorporating a DC–notch filter for eliminating sensitivity to DC offset.

The transfer function of a digital notch filter is given by a second order rational function with two parameters that characterize the location and width of the notch (see article by P. Regalia, S. K. Mitra and P. P. Vaidyanathan "The Digital All–Pass Filter: A Versatile Signal Processing Building Block," *PROCEEDINGS of the IEEE*, VOL.76, pp. 19–37, January 1988). The sensitivity of INPML detectors to DC offset can be eliminated by utilizing such

a filter with a notch at DC. It can be seen that the transfer function of a digital DC–notch filter is given by

$$H(D) = \frac{1+b}{2}\left[\frac{1-D}{1-bD}\right] \quad , \tag{13}$$

where b is a constant that determines the width of the notch. For a very narrow notch at DC, b must be chosen very close to unity. In this case, $(1 + b)/2 \approx 1$ and the transfer function of the notch filter simplifies to

$$H(D) = \frac{1-D}{1-bD} \quad . \tag{14}$$

Digital filters with a notch at DC are very simple to implement and do not require multipliers. Similarly, the transfer function of a DC–notch analog filter is given by

$$H(s) = \frac{s}{s+c} \quad , \tag{15}$$

where c is a constant that determines the width of the notch. For a very narrow notch c must be chosen very close to zero.

The DC–notch filter can be either imbedded into the INPML detector as part of the whitening IIR predictor or cascaded with the INPML detector. Figures 7A, 7B and 7C show the block diagrams of three possible configurations of an INPML detector with a DC–notch filter. In Fig. 7A, the notch filter 44a is included in the feedback path between the second output of the Viterbi detector 31 and its input, the path which also contains the IIR predictor 35. In the configuration of Fig. 7B, the notch filter 44b is inserted between the digital equalizer 22 and the INPML detector 10, and thus receives the samples y_n at its input. In the case of Fig. 7C, the notch filter 44c precedes the digital equalizer 22. Clearly, the same approach can be applied to other DC sensitive detectors such as NPML, non-adaptive DFE (decision feedback equalizer) and FDTS (fixed delay tree search) detectors. Summarizing, a DC–notch filter renders INPML :

–completely immune to DC offset,
–tolerant to MR (magneto–resistive) head asymmetry,
–tolerant to thermal asperities.

(b) Adaptive Asymmetry and DC Estimation Combined with INPML Detection :

An MR head is a nonlinear transducer that introduces asymmetry in the readback signal. Positive peaks can differ in amplitude from negative peaks by as much as 30 %. DC insensitive detectors such as PRML and INPML cascaded with a DC–notch filter are quite tolerant to small amounts of head asymmetry and suffer only a small performance degradation. The high losses in performance due to large amounts of head asymmetry can be recovered by an asymmetry estimation/compensation algorithm which is imbedded into the branch–metric computation of the INPML detector. Consider the following generic signal asymmetry model:

$$f(a_n,\ a_{n-2}) = \begin{cases} F_{+2} & \text{for} \quad a_n = 1 \text{ and } a_{n-2} = -1 \\ F_0 & \text{for} \quad a_n = a_{n-2} \\ F_{-2} & \text{for} \quad a_n = -1 \text{ and } a_{n-2} = 1 \end{cases}$$

Then, the branch metric computations of the 4–state INPML detector whose trellis is shown in Fig. 3 must be modified as follows:

$$\lambda_n(0,0) = |\, e_n(0,0) \,|^2 \quad \text{, where} \quad e_n(0,0) = y_n - F_0 + \tilde{w}_n(0)$$

$$\lambda_n(1,0) = |\, e_n(1,0) \,|^2 \quad \text{, where} \quad e_n(1,0) = y_n - F_{-2} + \tilde{w}_n(1)$$

$$\lambda_n(2,1) = |\, e_n(2,1) \,|^2 \quad \text{, where} \quad e_n(2,1) = y_n - F_0 + \tilde{w}_n(2)$$

$$\lambda_n(3,1) = |\, e_n(3,1) \,|^2 \quad \text{, where} \quad e_n(3,1) = y_n - F_{-2} + \tilde{w}_n(3)$$

$$\lambda_n(0,2) = |\, e_n(0,2) \,|^2 \quad \text{, where} \quad e_n(0,2) = y_n - F_{+2} + \tilde{w}_n(0)$$

$$\lambda_n(1,2) = |\, e_n(1,2) \,|^2 \quad \text{, where} \quad e_n(1,2) = y_n - F_0 + \tilde{w}_n(1)$$

$$\lambda_n(2,3) = |\, e_n(2,3) \,|^2 \quad \text{, where} \quad e_n(2,3) = y_n - F_{+2} + \tilde{w}_n(2)$$

$$\lambda_n(3,3) = |\, e_n(3,3) \,|^2 \quad \text{, where} \quad e_n(3,3) = y_n - F_0 + \tilde{w}_n(3)$$

The state metrics and feedback estimates at the next time instant $(n+1)T$ are computed as follows:

$$J_{n+1}(0) = min \{ J_n(0) + \lambda_n(0,0) \ , \ J_n(1) + \lambda_n(1,0) \}$$

$$\tilde{w}_{n+1}(0) = \begin{cases} \alpha \ e_n(0,0) \\ or \\ \alpha \ e_n(1,0) \end{cases}$$ Depending on whether state 0 or state 1 was the previous "winning" state

$$J_{n+1}(1) = min \{ J_n(2) + \lambda_n(2,1) \ , \ J_n(3) + \lambda_n(3,1) \}$$

$$\tilde{w}_{n+1}(1) = \begin{cases} \alpha \ e_n(2,1) \\ or \\ \alpha \ e_n(3,1) \end{cases}$$ Depending on whether state 2 or state 3 was the previous "winning" state

$$J_{n+1}(2) = min \{ J_n(0) + \lambda_n(0,2) \ , \ J_n(1) + \lambda_n(1,2) \}$$

$$\tilde{w}_{n+1}(2) = \begin{cases} \alpha \ e_n(0,2) \\ or \\ \alpha \ e_n(1,2) \end{cases}$$ Depending on whether state 0 or state 1 was the previous "winning" state

$$J_{n+1}(3) = min \{ J_n(2) + \lambda_n(2,3) \ , \ J_n(3) + \lambda_n(3,3) \}$$

$$\tilde{w}_{n+1}(3) = \begin{cases} \alpha \ e_n(2,3) \\ or \\ \alpha \ e_n(3,3) \end{cases}$$ Depending on whether state 2 or state 3 was the previous "winning" state

The values of the nonlinear function $f(a_n, a_{n-2})$ can be estimated for a particular head and media combination during manufacturing and then be used as fixed predetermined values in the branch metric computation unit of the INPML detector.

Alternatively, an algorithm that estimates these values dynamically can be used. Dynamic estimation can be achieved by a table look–up stochastic gradient algorithm which updates one memory location per time interval. Consider delayed decisions from the path memory of the INPML detector, say $\hat{a}_{n-d}$, $\hat{a}_{n-2-d}$. These decisions then form the address to the memory location of a RAM in which the corresponding values are stored. A simple schematic of a RAM with four memory locations containing corresponding values at time nT is shown in Figure 8. At the next time instant, $(n + 1)T$, the content of the

memory location addressed by $(\hat{a}_{n-d}, \hat{a}_{n-2-d})$ is updated according to the following algorithm:

$$\hat{f}_{n+1}(\hat{a}_{n-d}, \hat{a}_{n-2-d}) = \hat{f}_n(\hat{a}_{n-d}, \hat{a}_{n-2-d}) + \mu\, e_{n-d} \ ,$$

$$e_{n-d} = [\, y_{n-d} - \hat{f}_n(\hat{a}_{n-d}, \hat{a}_{n-2-d}) \,] \ ,$$

where y_{n-d} is the delayed, nonlinearly distorted received signal and μ is a small constant. The above algorithm can also be applied to remedy other forms of nonlinearity. In general, the number of symbols which the nonlinear function $f(.)$ depends on determines the size of the RAM.

The following asymmetry model has been used in the simulations:

$$f(a_n, a_{n-2}) = \begin{cases} 2 + 4\delta + DC = F_{+2} & \text{for} \quad a_n = 1 \text{ and } a_{n-2} = -1 \\ 0 + DC = F_0 & \text{for} \quad a_n = a_{n-2} \\ -2 + 4\delta + DC = F_{-2} & \text{for} \quad a_n = -1 \text{ and } a_{n-2} = 1 \ . \end{cases}$$

This model is basically a second–order nonlinearity coupled with a DC offset. In the simulations $\delta = 0.1$, i.e., 33% asymmetry, and $DC = 0.05$ have been chosen.

Performance of INPML detector with and without Asymmetry Compensation:

Figure 9 shows the error performance of a 4–state INPML detector with a single–pole predictor in the presence of electronic noise and head asymmetry for the channel model with $PW50/T \approx 2.86$. The head asymmetry is 33%. Curve 1 shows the performance of INPML without any asymmetry compensation. Curves 2 and 3 correspond to INPML combined with adaptive asymmetry estimation and $\mu = 0.05$ and $\mu = 0.005$, respectively. Finally, curve 4 shows the performance of INPML with ideal asymmetry estimation/compensation. These performance results show that the dynamic estimation methods can achieve the performance of ideal estimates.

Digital or Analog Implementations:

Note that, besides a fully digital implementation, the whole or portions of the elements shown in the INPML detector 10 of Fig. 2A/B, Fig. 4 and Fig. 7, can be implemented in analog circuit technology..

CLAIMS

1. Detector for encoded and uncoded data sequences having passed a partial–response equalizer, including means (10) for maximum likelihood sequence detection with noise prediction;

characterized in that it comprises:

– an infinite impulse response (IIR) noise predictor (35; 45) imbedded into the maximum likelihood sequence detection means.

2. Detector in accordance with claim 1, in which said infinite impulse response noise predictor (35) executes a transfer function $aD/(1 - aD)$, where a is a preselected scaling factor and D is the unit delay operator.

3. Detector in accordance with claim 1, in which said infinite impulse response noise predictor (45) executes a transfer function

$[-(\alpha_1 + \beta_1)D - (\alpha_2 + \beta_2)D^2]/[1 + \alpha_1 D + \alpha_2 D^2]$, where α_1, α_2, β_1, and β_2 are preselected scaling factors and D is the unit delay operator.

4. Detector in accordance with claim 2, in which

– said infinite impulse response noise predictor (35) is a single–pole filter comprising:

– an input (28) for noise samples ($\hat{w}_n$); an output (36) for predicted noise samples ($\tilde{w}_n$); first unit delay means (40) for delaying the input noise samples ($\hat{w}_n$); adding means (41) for adding the output of the first unit delay means and the output ($\tilde{w}_{n-1}$) of a second unit delay means (43); and multiplication means (42) for multiplying the output of said adding means (41) by a constant factor (α), furnishing to the output (36) the predicted noise samples ($\tilde{w}_n$); the second unit delay means (43) receiving at its input said predicted noise samples.

5. Detector in accordance with claim 3, in which

– said infinite impulse response noise predictor (45) is a double–pole and double–zero filter comprising:

– an input (28a) for noise samples ($\hat{w}_n$); an output (36a) for predicted noise samples ($\tilde{w}_n$); first and second unit delay means (47, 48) connected in series, for delaying the input samples ($\hat{w}_n$); first multiplication means (49) for multiplying the output of said second delay means by a first constant factor $[-(\alpha_2 + \beta_2)]$; adding means (50) for adding the output of said first multiplication means and correction terms appearing on further inputs (51, 52, 53) of said adding means, furnishing on its output (36a) the predicted noise samples ($\tilde{w}_n$); third and fourth unit delay means (55, 57) connected in series to the output of said adding means; and second, third and fourth multiplication means (54, 56, 58) for multiplying the outputs of said first (47), third (55) and fourth (57) unit delay means each by a respective constant factor ($[-(\alpha_1 + \beta_1)]; [-\alpha_1]; [-\alpha_2]$) and furnishing their outputs to said further inputs (51, 52, 53) of said adding means (50).

6. Detector in accordance with claim 4 or claim 5, in which

– subtracting means (46) are provided for furnishing said noise samples ($\hat{w}_n$) to the input (28; 28a) of said infinite impulse response noise predictor (35; 45);

– said subtracting means (46) having a first input (29) for reconstructed PR4 samples ($\hat{a}_n - \hat{a}_{n-2}$) and a second input (38) for equalized, noisy data samples (y_n); said subtracting means (46) forming the difference $\hat{w}_n$ of the noisy data samples and the reconstructed PR4 samples.

7. Detector in accordance with claim 6, further including:

– means (34) for reconstructing PR4 data samples ($\hat{a}_n - \hat{a}_{n-2}$) by a transfer function $(1 - D^2)$, the input of the reconstructing means being connected to the path history of a Viterbi detector (31) providing path history decisions ($\hat{a}_n$), and its output (29) being connected to the first input (29) of the subtracting means (46).

8. Detector in accordance with claim 1, in which the filter function of said infinite impulse response noise predictor (35; 45) has not more than two poles and not more than two zeros.

9. Detector in accordance with claim 1, further comprising

– a DC–notch filter (44), either imbedded in, or cascaded with, the maximum likelihood detection means (10) which comprises the infinite impulse response noise predictor (35; 45), for DC offset compensation.

10. Detector in accordance with one of the preceding claims 1 through 9, in which

– at least a portion of said maximum likelihood detection means (10) which comprises the infinite impulse response noise predictor (35; 45), is implemented in analog circuit technology.

11. Detection method for encoded or uncoded data sequences having passed a partial–response equalizer, based on maximum likelihood sequence detection with noise prediction;

characterized by:

– an infinite impulse response (IIR) noise prediction procedure integrated with the maximum likelihood sequence detection process.

12. Detection method in accordance with claim 11, in which said infinite impulse response noise prediction filters the difference ($\hat{w}_n$) between partial–response equalized, noisy samples (y_n) and reconstructed samples ($\hat{a}_n - \hat{a}_{n-2}$) derived from the output of a maximum likelihood detection process, and provides predicted noise samples ($\tilde{w}_n$).

13. Detection method in accordance with claim 11 or claim 12, in which

– the infinite impulse response noise prediction procedure executes a transfer function $aD/(1 - aD)$, where a is a preselected scaling factor and D is the unit delay operator.

14. Detection method in accordance with claim 11 or claim 12, in which

– the infinite impulse response noise prediction procedure executes a transfer function $[-(\alpha_1+\beta_1)D-(\alpha_2+\beta_2)D^2]/[1+\alpha_1 D+\alpha_2 D^2]$, where α_1, α_2, β_1, and β_2 are preselected scaling factors and D is the unit delay operator.

15. Detection method in accordance with claim 11, in which said infinite impulse response noise prediction procedure is executed multiple times, once for each state of the trellis of the maximum likelihood sequence detection process.

16. Detection method in accordance with claim 11, including

– a procedure for DC offset compensation and reading head asymmetry compensation, comprising following steps:

– addressing a memory containing estimates $\hat{f}(.)$ of a nonlinearity, using delayed decisions $\hat{a}_{n-d}$ as addresses, and using the nonlinearity signal estimate values thus obtained from the memory, in the branch metric computation for each state of the maximum likelihood sequence detection process which includes the infinite impulse response noise prediction procedure; and

– concurrently, updating the estimates of the nonlinearity $\hat{f}(.)$ contained in the memory, by a stochastic gradient procedure according to

$$\hat{f}_{n+1}(\hat{a}_{n-d},\hat{a}_{n-2-d}) = \hat{f}_n(\hat{a}_{n-d},\hat{a}_{n-2-d}) + \mu\, e_{n-d}$$

$$e_{n-d} = [\, y_{n-d} - \hat{f}_n(\hat{a}_{n-d},\hat{a}_{n-2-d})\,]\,.$$

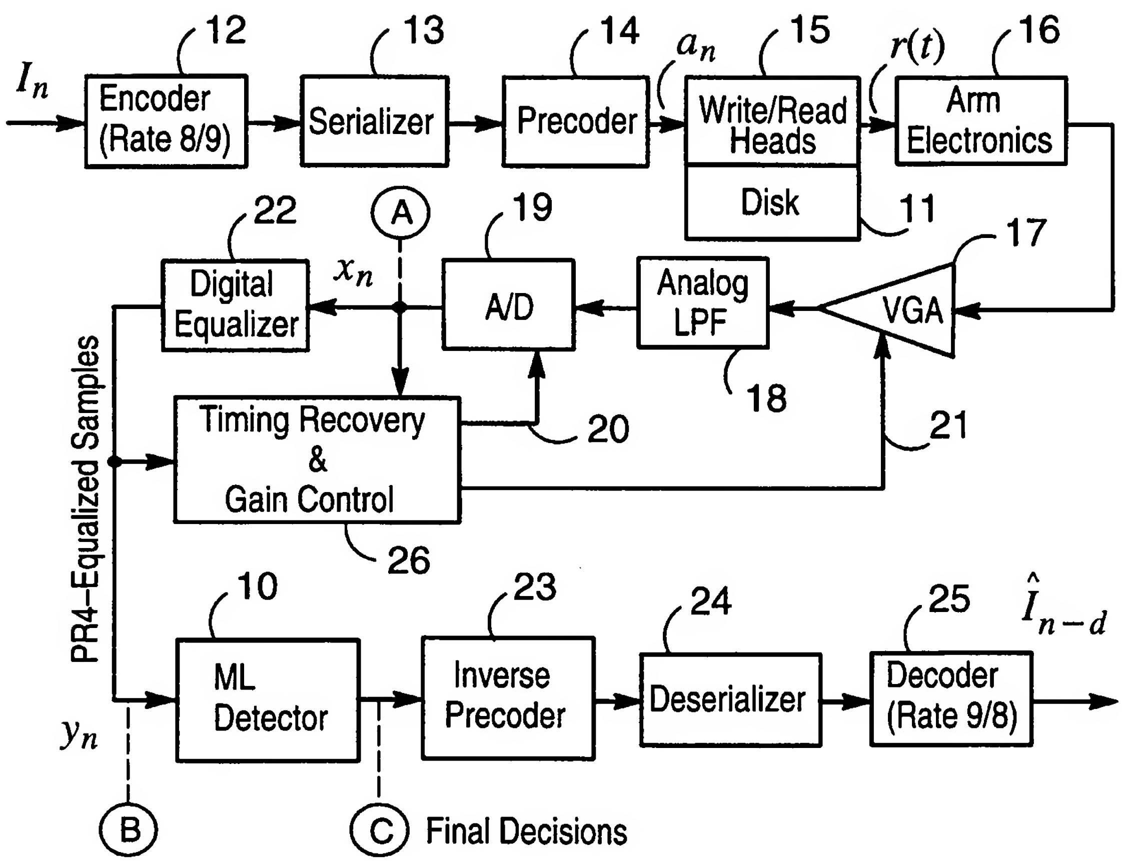

I_n
12
Encoder (Rate 8/9)
13
Serializer
14
Precoder
a_n
15
Write/Read Heads
Disk
11
$r(t)$
16
Arm Electronics
17
VGA
18
Analog LPF
19
A/D
A
x_n
22
Digital Equalizer
Timing Recovery & Gain Control
20
21
26
PR4–Equalized Samples
10
ML Detector
23
Inverse Precoder
24
Deserializer
25
Decoder (Rate 9/8)
$\hat{I}_{n-d}$
y_n
B
C
Final Decisions

FIG. 1

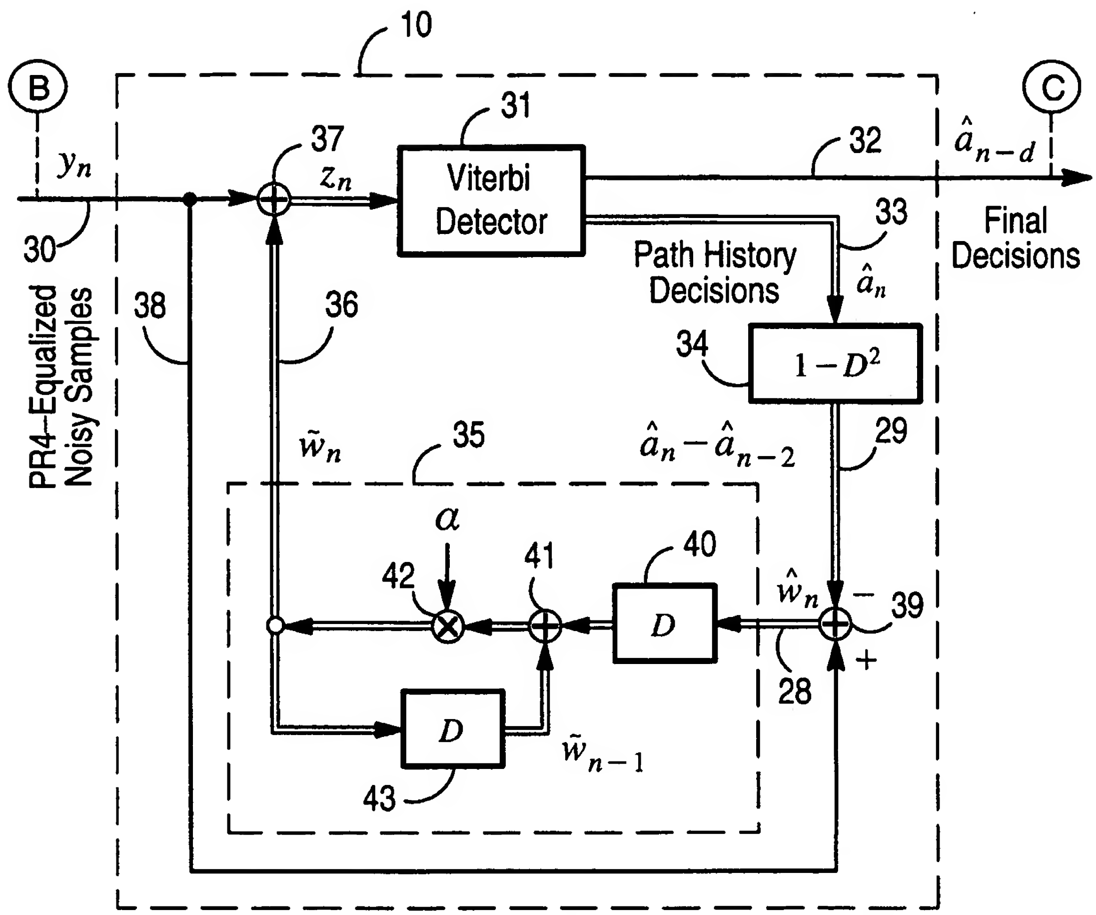

10
B
C
y_n
30
PR4–Equalized Noisy Samples
37
z_n
31
Viterbi Detector
32
$\hat{a}_{n-d}$
Final Decisions
33
Path History Decisions
$\hat{a}_n$
34
$1-D^2$
38
36
$\tilde{w}_n$
35
$\hat{a}_n - \hat{a}_{n-2}$
29
α
42
41
40
D
$\hat{w}_n$
−
39
+
28
D
$\tilde{w}_{n-1}$
43

FIG. 2A

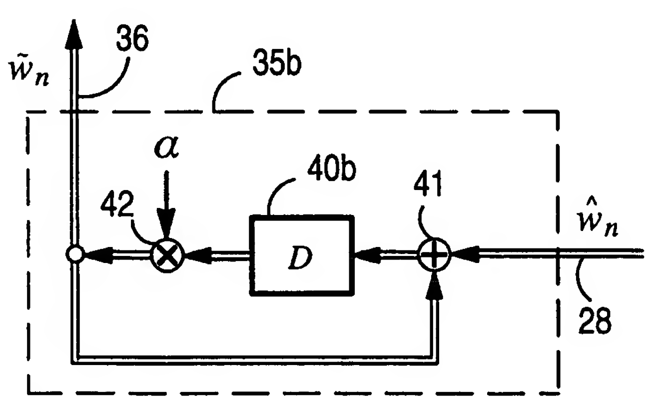

36
$\tilde{w}_n$
35b
α
40b
41
42
D
$\hat{w}_n$
28

FIG. 2B

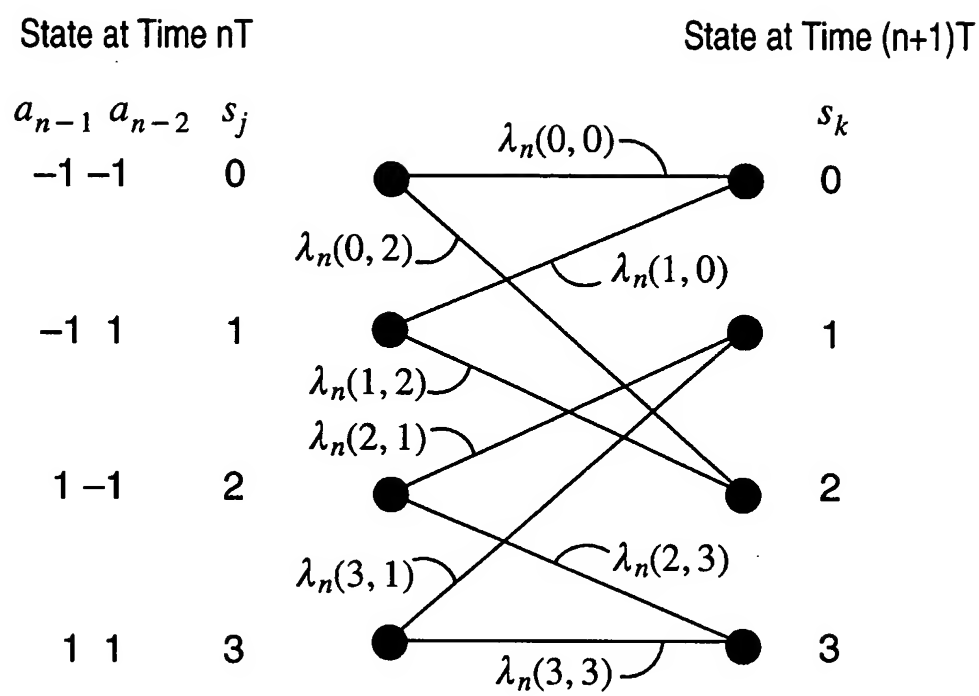
State at Time nT
State at Time (n+1)T
a_{n-1} a_{n-2} s_j
–1 –1 0
–1 1 1
1 –1 2
1 1 3
s_k
0
1
2
3
$\lambda_n(0,0)$
$\lambda_n(0,2)$
$\lambda_n(1,0)$
$\lambda_n(1,2)$
$\lambda_n(2,1)$
$\lambda_n(2,3)$
$\lambda_n(3,1)$
$\lambda_n(3,3)$

FIG. 3

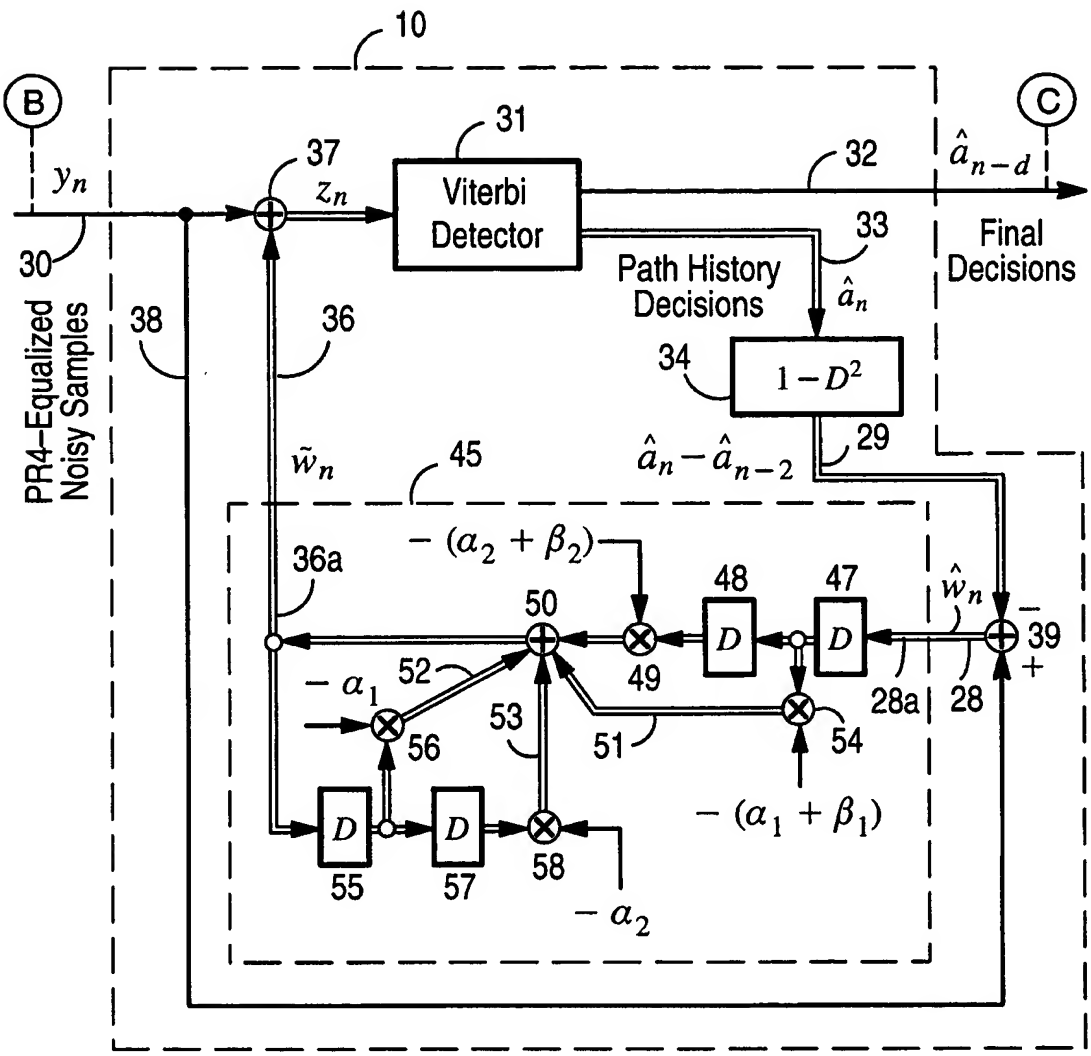
10
B
C
y_n
30
PR4–Equalized Noisy Samples
37
z_n
31
Viterbi Detector
32
$\hat{a}_{n-d}$
Final Decisions
33
Path History Decisions
$\hat{a}_n$
34
$1-D^2$
29
$\hat{a}_n - \hat{a}_{n-2}$
38
36
$\tilde{w}_n$
45
36a
$-(\alpha_2+\beta_2)$
48
47
$\hat{w}_n$
50
D
D
49
39
28a
28
52
$-\alpha_1$
56
53
51
54
$-(\alpha_1+\beta_1)$
55
57
58
$-\alpha_2$

FIG. 4

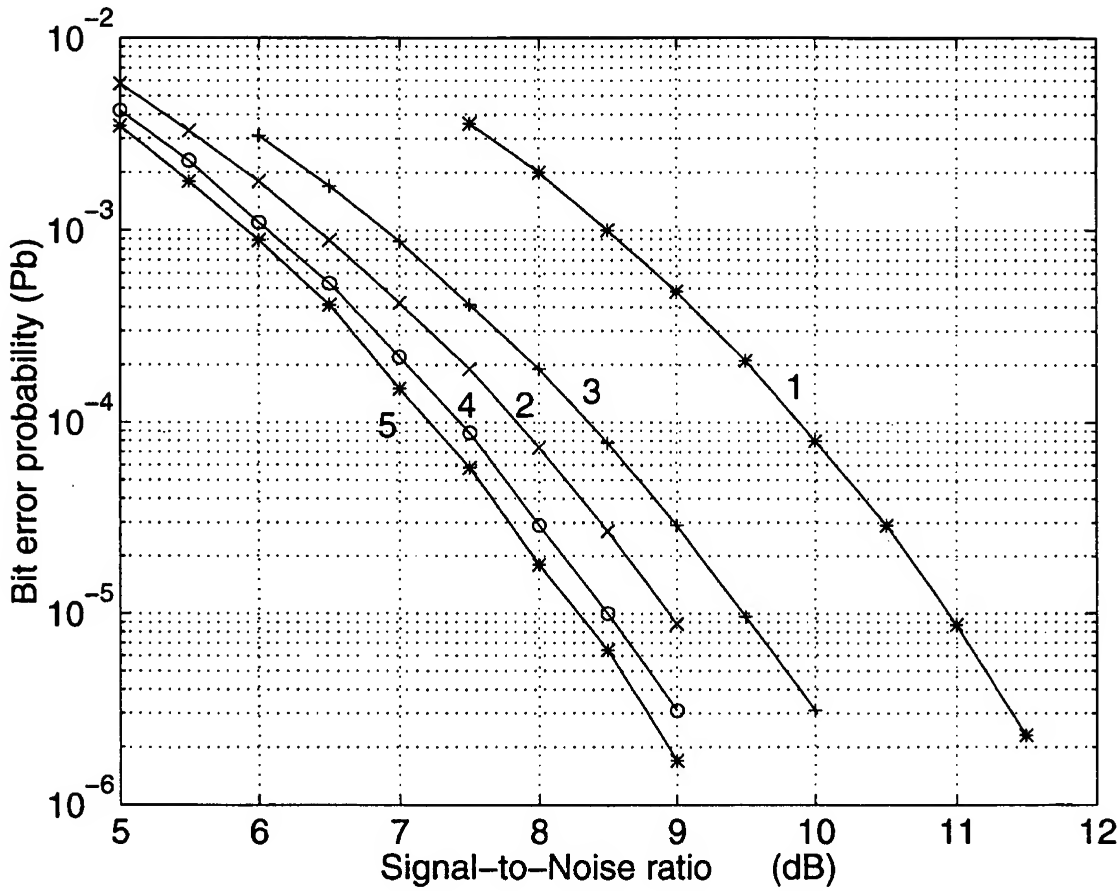
10^-2
10^-3
10^-4
10^-5
10^-6
Bit error probability (Pb)
5
6
7
8
9
10
11
12
Signal-to-Noise ratio (dB)
1
2
3
4
5

FIG. 5

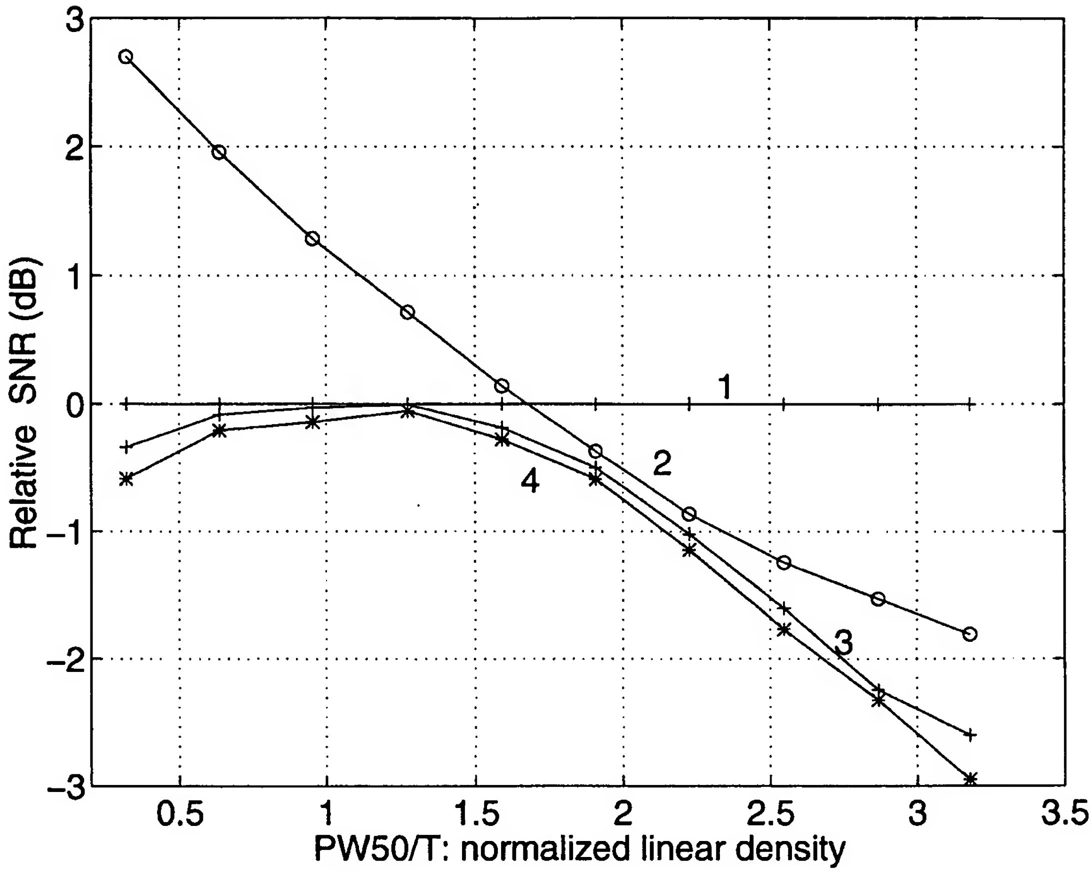
3
2
1
0
−1
−2
−3
Relative SNR (dB)
0.5
1
1.5
2
2.5
3
3.5
PW50/T: normalized linear density
1
2
3
4

FIG. 6

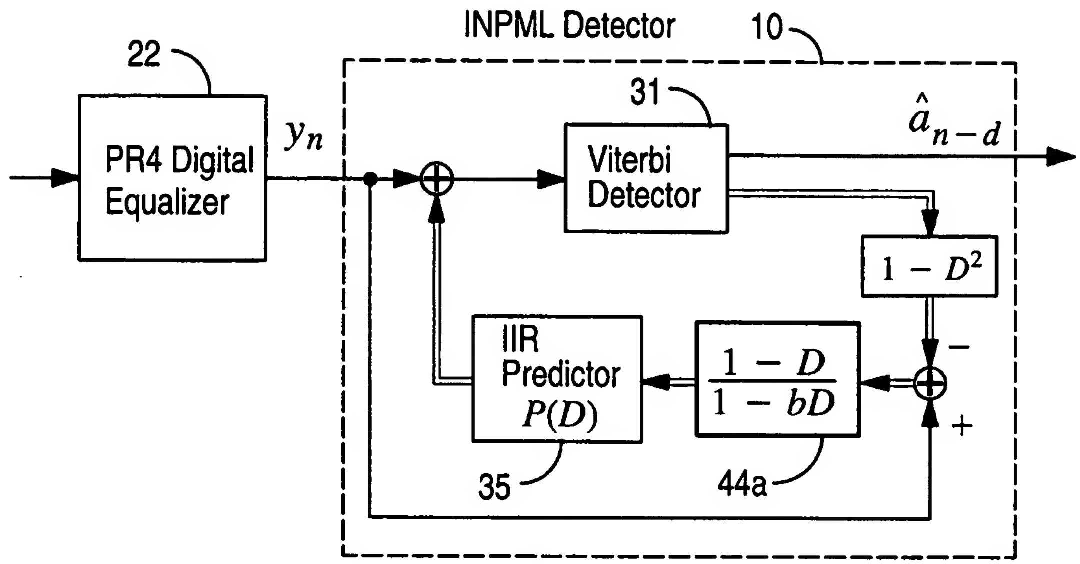

FIG. 7A

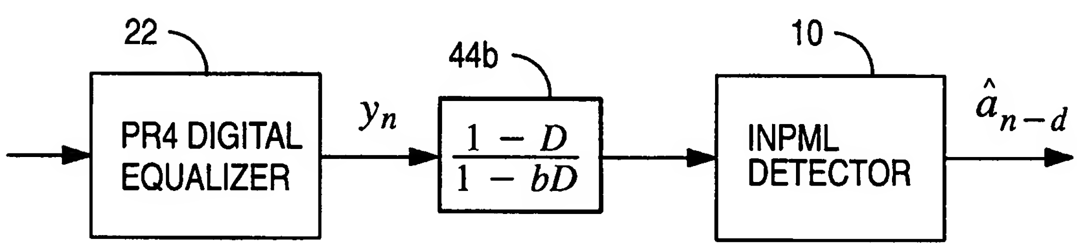

FIG. 7B

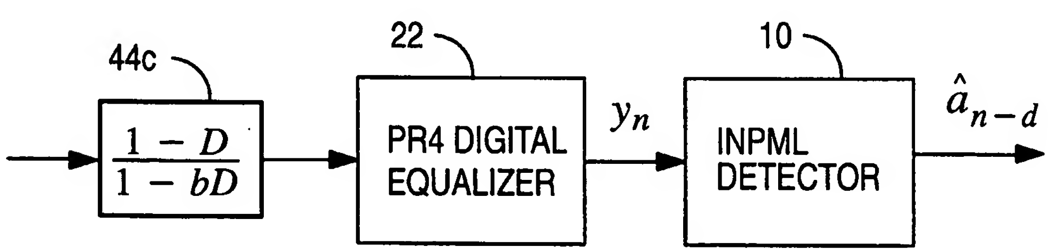

FIG. 7C

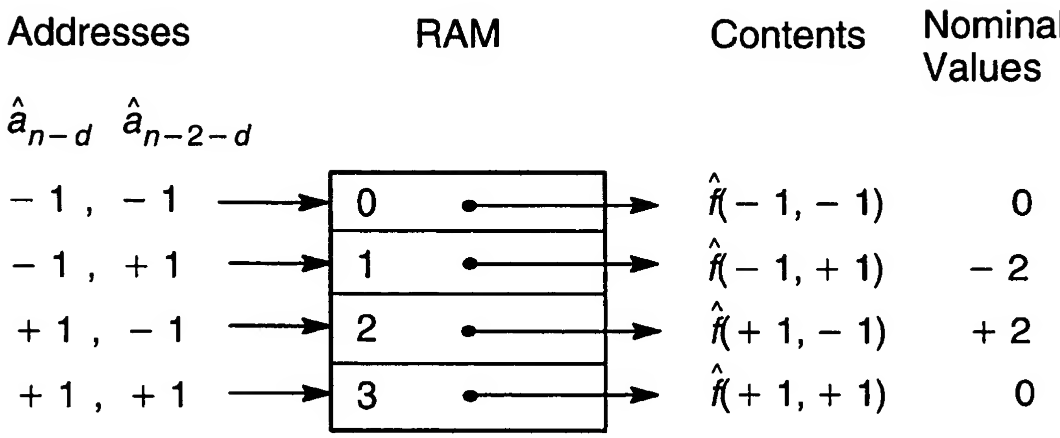
Addresses
RAM
Contents
Nominal Values
$\hat{a}_{n-d}$ $\hat{a}_{n-2-d}$
− 1 , − 1
− 1 , + 1
+ 1 , − 1
+ 1 , + 1
0
1
2
3
$\hat{f}(-1,-1)$
$\hat{f}(-1,+1)$
$\hat{f}(+1,-1)$
$\hat{f}(+1,+1)$
0
− 2
+ 2
0

FIG. 8

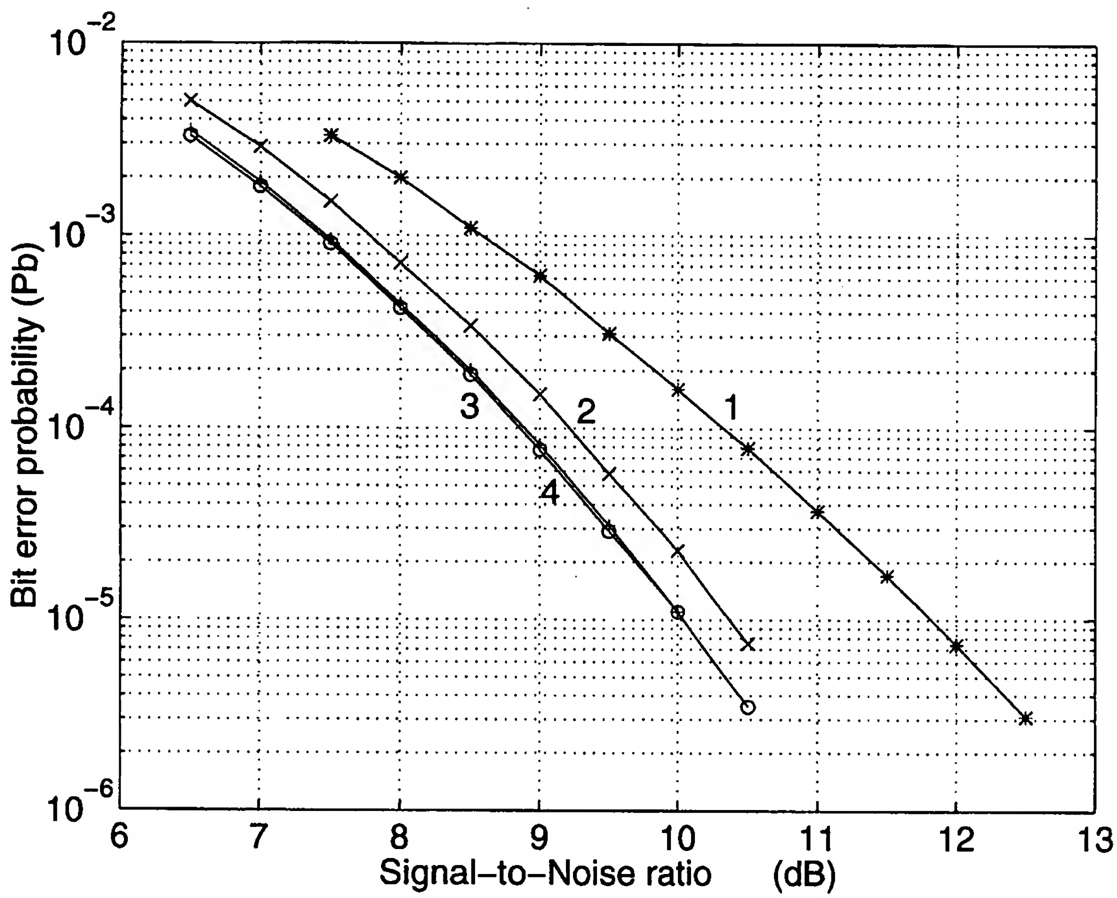
10^{-2}
10^{-3}
10^{-4}
10^{-5}
10^{-6}
Bit error probability (Pb)
6
7
8
9
10
11
12
13
Signal-to-Noise ratio (dB)
1
2
3
4

FIG. 9

INTERNATIONAL SEARCH REPORT

Interr nal Application No
PCT/IB 97/00554

A. CLASSIFICATION OF SUBJECT MATTER
IPC 6 H04L25/03 H04L25/497

According to International Patent Classification(IPC) or to both national classification and IPC

B. FIELDS SEARCHED

Minimum documentation searched (classification system followed by classification symbols)
IPC 6 H04L

Documentation searched other than minimum documentation to the extent that such documents are included in the fields searched

Electronic data base consulted during the international search (name of data base and, where practical, search terms used)

C. DOCUMENTS CONSIDERED TO BE RELEVANT

Category °	Citation of document, with indication, where appropriate, of the relevant passages	Relevant to claim No.
A	WO 97 11544 A (IBM) 27 March 1997 cited in the application see abstract see figure 2D ---	1-16
A	CHEVILLAT P R ET AL: "NOISE-PREDICTIVE PARTIAL-RESPONSE EQUALIZERS AND APPLICATIONS" INTERNATIONAL CONFERENCE ON COMMUNICATIONS, ICC'92, CHICAGO, US, vol. 2 OF 4, 14 - 18 June 1992, INSTITUTE OF ELECTRICAL AND ELECTRONICS ENGINEERS, pages 942-947, XP000326811 see section II see figure 1 --- -/--	1-16

[X] Further documents are listed in the continuation of box C.

[X] Patent family members are listed in annex.

° Special categories of cited documents :

"A" document defining the general state of the art which is not considered to be of particular relevance

"E" earlier document but published on or after the international filing date

"L" document which may throw doubts on priority claim(s) or which is cited to establish the publication date of another citation or other special reason (as specified)

"O" document referring to an oral disclosure, use, exhibition or other means

"P" document published prior to the international filing date but later than the priority date claimed

"T" later document published after the international filing date or priority date and not in conflict with the application but cited to understand the principle or theory underlying the invention

"X" document of particular relevance; the claimed invention cannot be considered novel or cannot be considered to involve an inventive step when the document is taken alone

"Y" document of particular relevance; the claimed invention cannot be considered to involve an inventive step when the document is combined with one or more other such documents, such combination being obvious to a person skilled in the art.

"&" document member of the same patent family

Date of the actual completion of the international search	Date of mailing of the international search report
21 January 1998	28/01/1998

1

Name and mailing address of the ISA	Authorized officer
European Patent Office, P.B. 5818 Patentlaan 2 NL - 2280 HV Rijswijk Tel. (+31-70) 340-2040, Tx. 31 651 epo nl, Fax: (+31-70) 340-3016	Ghigliotti, L

INTERNATIONAL SEARCH REPORT

Interr nal Application No
PCT/IB 97/00554

C.(Continuation) DOCUMENTS CONSIDERED TO BE RELEVANT

Category °	Citation of document, with indication,where appropriate, of the relevant passages	Relevant to claim No.
A	DUEL-HALLEN A ET AL: "DELAYED DECISION-FEEDBACK SEQUENCE ESTIMATION" IEEE TRANSACTIONS ON COMMUNICATIONS, vol. 37, no. 5, May 1989, pages 428-436, XP000670554 cited in the application see the whole document ---	1-16
A	MOHAMMAD GHAVAMI ET AL: "DECISION FEEDBACK EQUALIZATION OF HDSL USING A GENERALIZED ADAPTIVE IIR DELAY FILTER" EUROPEAN TRANSACTIONS ON TELECOMMUNICATIONS AND RELATED TECHNOLOGIES, vol. 5, no. 3, 1 May 1994, pages 37/337-46/346, XP000456626 see section 2 see figure 1 -----	1-16

1

INTERNATIONAL SEARCH REPORT

..ormation on patent family members

Interr nal Application No
PCT/IB 97/00554

Patent document cited in search report	Publication date	Patent family member(s)	Publication date
WO 9711544 A	27-03-97	NONE	

Form PCT/ISA/210 (patent family annex) (July 1992)